King's Research Portal

[Link to publication record in King's Research Portal](#)

Arresting High-Temperature Microstructural Evolution inside Sintered Silver

Khalid Khtatba*[1], Seyed Amir Paknejad [1], Tariq Al Zoubi [2], Hamzeh Qutaish [3], Naoko Sano[4,] Samjid H. Mannan[1]

[1] King's College London, Physics Department, Strand, London, WC2R 2LS, UK

[2] College of Engineering and Technology, American University of the Middle East (AUM), Kuwait

[3]Australian Institute for Innovative Materials (AIIM), University of Wollongong (UOW), Squires Way, North Wollongong, NSW, 2500, Australia

[4]Clothing Environmental Science, Division of Human Life and Environmental Sciences, The National University Corporation Nara Women's University, Nisi-machi, Kita Uoya, Nara, 630-8506, Japan

*Tel: +44 (0) 7588804321 Email: khalid.khtatba@kcl.ac.uk

Abstract:

The surface oxidation of internal pore surfaces of nano-scale sintered silver has increased stability for high temperature applications. Operating temperatures of up to 400 °C have resulted in no or minimal changes in microstructure. By contrast, it is known that the microstructure of untreated pressure-less sintered silver continuously evolves at temperatures above 200 °C, grain and pore growth resulting in microstructure coarsening and increased susceptibility to fatigue. Oxidation of the internal pore surfaces has been shown to freeze the microstructure when the contact metallization is also silver or chemically inert. Samples exhibited no change in microstructure either through continuous observation through glass, or after cross sectioning. The tested specimens under high temperature storage resisted grain growth for more than 1000 h at 300 °C. The oxidising treatment can be performed via many different routes. For example, exposure to steam, or even by dipping in water for 10 min followed by immediate high temperature exposure and the effectiveness of these varying treatments is assessed. In this work we explore the mechanism that causes stabilization and explore the hypothesis that oxidation prevents grain boundary movements by arresting the fast migration of atoms along the internal pore surfaces. Analysis of the surface structure of the sintered silver by x-ray photoelectron spectroscopy (XPS)

shows presence of silver oxide (Ag$_2$O) and computer simulation of grain boundary movements confirm the presence of a barrier to atomic movement on the internal silver surfaces. These findings are very promising for potential applications of sintered silver as a die attach material for High Temperature electronics packaging.

Keywords: Electronic Packaging, Sintering, Bonding, Aging, Die Attach, Nanoscale Silver, High Temperature.

1. Introduction

The die attach material remains one of the most important reliability concerns for high temperature electronics applications at temperatures of 300 °C and higher [1]. These applications include jet engines, oil and gas well drilling/monitoring, geothermal energy, and general wide-bandgap semiconductors for power applications, for which 400 ℃ is targeted for near future [2] While materials such as high melting point solders and solid liquid inter diffusion bonding systems exist, they suffer from inherent drawbacks, which make them less attractive for the high temperature community[3][4] Therefore, there has been significant interest in decoupling the melting point and processing temperature of die attach materials through use of nanoparticles, especially nano-sized silver [5], which typically sinter at temperatures under 300 °C but thereafter retain the properties of the bulk metal. Their low sintering temperature being due attributed to the high surface energy of the nanoparticles. In this paper, a method of increasing the stability of existing sintered silver materials is described, and the mechanism responsible for increasing the stability examined.

Sintered silver goes through massive grain structure changes at temperatures above 200 ℃, introducing uncertainty regarding the suitability of sintered silver for high temperature application due to evolution of material parameters in service and reduced shear strength[6] [7]. One attempt to increase the thermal stability of sintered silver uses a gold mesh interposer [8], and another utilizes addition of SiC [9]. The method described in this work stabilizes sintered silver without addition of other secondary materials or complex manufacturing steps [10][11]. Cleaning

electronics by water dipping is a standard method used for electronics cleaning without any moisture absorption-related risks [12]. Figure 1 describes the main steps of the method first introduced in reference [11], consisting of pressure-less sintering in air, followed by penetration of an oxidizing agent into the porous silver structure after sintering. In this work a number of methods of introducing the oxidizing step have been examined and the temperature-time stability limits resulting from this technique have been determined. The presence and identification of the oxide layer on sintered silver has been carried out using XPS. COMSOL Multiphysics® software has been utilised in an attempt to further understand the effects of an oxide layer by modelling the diffusion behaviour and resulting microstructural evolution of individual grains in the absence of an oxide. While there have been empirical studies to investigate the microstructural evolution inside sintered silver previously [13][6], these have not probed the underlying mechanisms. A few studies have been carried out on the modelling of its long-term reliability using Finite Element (FE) methods, using visco-plastic continuum mechanics models[14], again without detailed understanding of the underlying mechanisms.
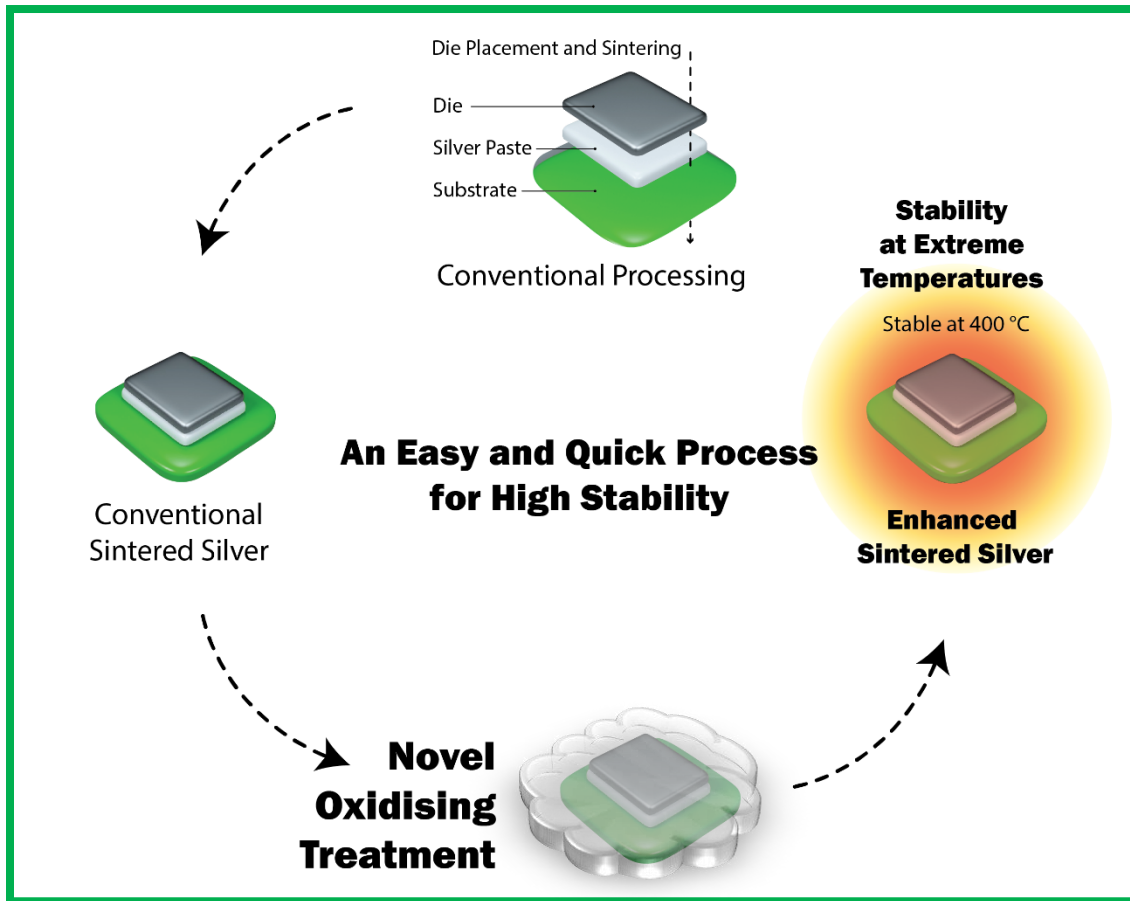
Figure 1. An easy processing step to increase thermal stability of sintered silver to 400 °C.

In general, looking at non-metallic materials such as ceramics, there are a large number of studies simulating the behaviour of micron scale particles during sintering (e.g.[15][16]) along with other studies simulating the initial sintering behaviour of nanoparticles, including silver nanoparticles (e.g. [17]17]) using both molecular dynamics and phase field approaches. However, there exists a lack of studies on the microstructural evolution of sintered nanoparticles during thermal ageing after the initial sintering process is complete. While, there are some studies of microstructural evolution aimed at capturing the microstructural evolution of grains of ceramic materials [18][19][20], simulating high temperature ageing behavior of sintered silver nanoparticles has not been investigated previously. It has been noted that if surface diffusion dominates over grain boundary diffusion that the evolution behavior will be different from normal evolution patterns [18], and sintered silver evolution is of particular interest because while a pure silver surface would

indeed exhibit high surface diffusion, a heavily oxidized silver surface would be expected to behave differently[6]. A priori, the condition of the interior sintered silver surfaces cannot be predicted as the reactions with chemicals in the original silver nanoparticle paste, and with oxygen diffusing in from the external atmosphere create an unpredictable environment. Nevertheless, predictions of microstructural evolution during ageing are important as unlike solders, no extensive knowledge base of how to predict long term behavior of sintered silver on the basis of accelerated testing currently exists. Therefore, the purpose of the modelling described in this work is to introduce a simple model to further increase the understanding of the microstructural evolution at high temperatures. The reliability of these simulations has been then tested using a new experimental setup to observe the real microstructural evolution of silver at high temperatures without exposure of sintered silver to atmosphere.

In order to compare the modelling results with experimental observation, the method described in reference [6] is used to study the evolution of individual grains at 350 and 387 °C. The method consists of observing individual grains optically through a glass cover slip. The computer simulation of these grains using COMSOL Multiphysics® software is then compared with the experimental results. The advantage of this simulation technique is that it can provide a more cost effective and convenient alternative than real-time ageing for predicting the changes that will occur.

2. Material and Methods

2. A) Sintered Silver Stabilisation

It has been previously shown that sintered silver can be stabilised through exposure to steam, and it has also been revealed that placing the sintered silver in water before exposure to high temperatures provides the same effect [10][11]. In the previous studies the treated samples have demonstrated stability up to at least 600 h at 300 °C, and up to at least 24 h at 350 °C and 400 °C. One of the aims of this work is to place more precise limits on these figures.

Silver nanoparticle paste from NBE Tech, LLC, NanoTach® X-Paste was chosen for this work due to the numerous previous studies of this and similar systems [10]. The material is

recommended for die sizes of up to 10×10 mm with a pressure-less sintering process, and peak sintering temperature of 255 C° for 25 minutes. The paste was used for attachment of a cover-slip to a glass slide by utilising the recommended temperature profile inside an oven (Lenton LC04-1.06) in air, corresponding to the normal sintering step for this material. Next the samples were placed alongside an open beaker containing 500 mL of water inside a sealed container, and the container was replaced inside the oven to perform the steaming process. The standard steaming step was 150 °C for 24 h, but variations of these times and temperatures were investigated, together with alternative treatments such as immersion into water and hydrogen peroxide, as described in Table 1.

After the various treatments, samples were stored at 300, 350, 400 and 450 °C. After various time intervals, the samples were removed to non-destructively check for any changes to the microstructure by observation with an optical microscope through the cover slip. Details of the treatments, storage conditions, and evidence of microstructural changes are given in Table 1. The grain sizes were analysed by taking optical images of the samples and analysing the average grain sizes of the samples using ImageJ 1.46 and the Matlab® image processing toolbox. Detailed description of grain size calculations can be found in references [10],[13]. The measured average grain sizes were then investigated to estimate the limitations of the sintered silver stabilisation technique at each storage temperature.

Another set of experiments using the same materials as for the ageing experiments described above were carried out to provide experimental data to compare to the computer simulations. These required in-situ observation of grain growth at elevated temperatures, and the experimental setup is shown in Figure 2. One sample was heated to 350 °C and another to 387 °C using a cartridge heater, and the temperature was then kept constant. Images of the sintered silver's structure are taken in-situ and continuously from the samples.
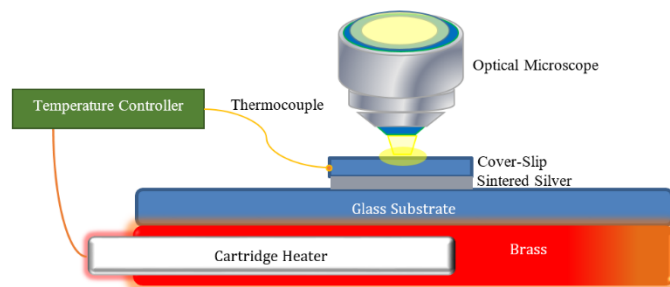
Fig. 2. Experimental setup's schematic representation. (Cartridge heater was inserted inside the brass)

2b) Materials Analysis (XPS, DSC)

X-ray photoelectron spectroscopy (XPS) is a spectroscopic technique which has an application in analysis of the composition of chemical surfaces, electronic state, chemical state and empirical formula of the compounds that form the material at the concentration range of parts per thousand. The X-ray beam is used to obtain a spectra and concurrently measures the emission of electrons from the surface (0 to 10nm) of the material being analyzed and also the kinetic energy. XPS involves the use of high vacuum[21].

Al-KαX-ray source (Thermo Scientific) was used to investigate the chemical composition up to 10 nm depth for one samples. A silver nanoparticle based paste labeled X-paste from NBE Tech was used. The sample were sintered at 255°C for 25 minutes, using glass substrate. The sample were made 24 hours before the XPS experiment was run. CASPXPS software been used to analyses the data. For the Differential Scanning Calorimeter (DSC) model under the name Mettler Toledo DSC 822e/STARe was used, along with aluminum pans for specimen encapsulation (AL-crucibles 40μl model (ME-26763) and a manual press was used for covering the pans.

Sample Set	Sample Number	Treatment	High Temperature Aging (°C)	Aging Time (hours)	Changes
	1.1		No Aging	No Aging	(Control)
	1.2		200	5	No
1	1.3	Untreated	250	7	Yes
	1.4		300	7	Yes
	1.5		350	7	Yes
	1.6		400	7	Yes
	2.1		300	24	No
	2.2		300	100	No
	2.3		300	500	No
	2.4		300	600	No
	2.5		300	1008	No
	2.6	Steam	350	24	No
2	2.7	(150 °C / 24 h)	350	72	No
	2.8		350	144	Yes (Edge)
	2.9		350	168	Yes (Edge)
	2.10		350	336	Yes
	2.11		400	24	No
	2.12		400	48	Yes
	2.13		450	1	No
	2.14		450	24	Yes
	3.1	1 h water / 1 h steam	300	24	No
3	3.2	Only 1 h water	300	24	No
	3.3	10 min water	300	24	No
	3.4	10 min water/24 h drying	300	24	Yes (Random)
4	4.1	10 % Hydrogen Peroxide 60 °C / 24 h dry	300	24	No

Table 1 consisting of sample set labels, treatments, ageing conditions and the presence of microstructural changes.

2c) **COMSOL Simulation**

For simulations COMSOL Multiphysics® 5.2a has been utilized in 2D. In this study, the main driver of microstructural change is assumed to be curvature relaxation as atoms diffuse along surfaces to minimise their chemical potential, lowering the total free energy in the system by decreasing surface area. This phenomenon can be simplified into the form of a normal velocity to the surface of the particle [22] , allowing the change in position of the particle surface to be tracked. Eq. (1) below in Cartesian coordinates represents the relationship between the curvature relaxation and this normal velocity:

$$v_n = \frac{D_S\, X_S \gamma\, \Omega^2}{k_B\, T}\, \left(\frac{\partial^2 K}{\partial x^2} + \frac{\partial^2 K}{\partial y^2}\right) \qquad\qquad (1)$$

where v_n is the normal velocity of the surface of the particle at any given point on its surface (m/s), D_S is the surface diffusion (m²/s), X_S is the surface atomic density (atom/m²), γ is the surface energy (J/m²), Ω is the atomic volume (m³/atom), k_B is the Boltzmann constant (J/K), T is the temperature of the particle (K), and K is the curvature at any point on the surface (1/m), see Table 2 for their values.

Table 2: Values of variable used for calculation of v_n.

Variable	Sample at 350 °C	Sample at 387 °C
D_S	0.91E-8 m²/s [24]	1.10E-8 m²/s [24 sim]
X_S	2.39E19 atom/m²	2.39E19 atom/m²
γ	890 mJ/m² [25]	890 mJ/m² [25 sim]
Ω	1.71E-29 m³/atom	1.71E-29 m³/atom
k_B	1.38E-23 J/K	1.38E-23 J/K
T	623 K	660 K

To input Eq. (1) into COMSOL two main modules were utilized. Initially, the General Form PDE

(Partial Differential Equation) module was used to calculate the values of v_n by differentiating the curvature on the surface. Then, the calculated values were inserted into the Moving Mesh module to yield the changes of the particles' shape. For our comparison two silver grains have been selected, one from the 350 °C experiment and another from the 387 °C study. The initial geometry of each grain was created and then simulated in COMSOL to investigate and compare experimental results and the theoretical changes that should occur on oxide-free pure silver surfaces.

3. Results and Discussion

a. Sintered Silver Stabilisation

If no stabilizing treatment is applied, the microstructure evolves and coarsens over time as seen in Fig.3. Figure 3 and subsequent figures show images which all represent the interior of the sample except for samples aged at 350 °C where a different microstructure was observed at the edges. Images from the edges are explicitly labelled in Fig.7. The previously determined limits of the steaming technique were stability for at least 600 h at 300 °C and at least 24 h at 350 and 400 °C. Table 1 indicates that the stabilisation technique can prevent changes for at least 1008 h at 300 °C, and up to 77 h at 350 °C, up to 24 h at 400 °C and up to 1 h at 450 °C. Figure 3 shows the qualitative changes occurring at these temperatures and ageing times. Treated samples up to 300 °C remained stable for the duration of the experiment. Figure 4 quantifies the average grain size of sintered silver before storage at temperatures ranging from 300 to 400 °C. Figure 5 indicates the maximum time that treated sintered silver can resist high temperature microstructural evolution.

Figure 6 outlines the geometry of the experiment indicating which the location of "central" and "edge" areas of the sintered silver since the 350 ℃ experiments allow the progressive breakdown of the stability to be mapped across the sample. Figures 7-9 show that at 350 °C the edges of the sample show weak grain growth at 144 h, and strong grain growth at 200 h, while the central areas remain stable. The experiment was stopped when grain growth was observed everywhere inside the sample, at 336 h. These changes have been shown quantitatively in Fig.10 which shows a comparison of the central grain sizes with the grain sizes on the edges of the samples. The 400 °C sample also exhibits a similar trend. The edges of the samples show grain growth after 48 h storage.

The initial grain growth starting from the edges might be related to the larger free surface area of the grains on the edges, since previous research indicates that there is a finer grain structure at the edges [23], allowing the external grains to start the grain growth by absorption of the smaller grains and allowing this trend to continue internally. However, it seems more likely that the contact of the outer grains with the ambient atmosphere is responsible for the breakdown of the stabilizing layer. Chemical reactions between the oxygen or water vapour or other contaminants in the air (e.g. sulphur) and the stabilizing layer on the sintered silver could be responsible for the breakdown on the edges of the samples. Previous research [24] shows that the pores in pressure-less sintered silver form an open network and hence diffusion of air throughout the structure could explain the pattern of breakdown of protection at 350 °C and higher. Indeed, the very presence of the barrier layer indicates that the network must be open as otherwise steam would not have been able to penetrate into the interior of the sample. Table 1 indicates that immersing the sintered silver into liquid water or hydrogen peroxide also cause a protective barrier to form. The only treatment that failed was sample 3.4 which allowed the water to dry out before heat treatment could turn the water into steam.
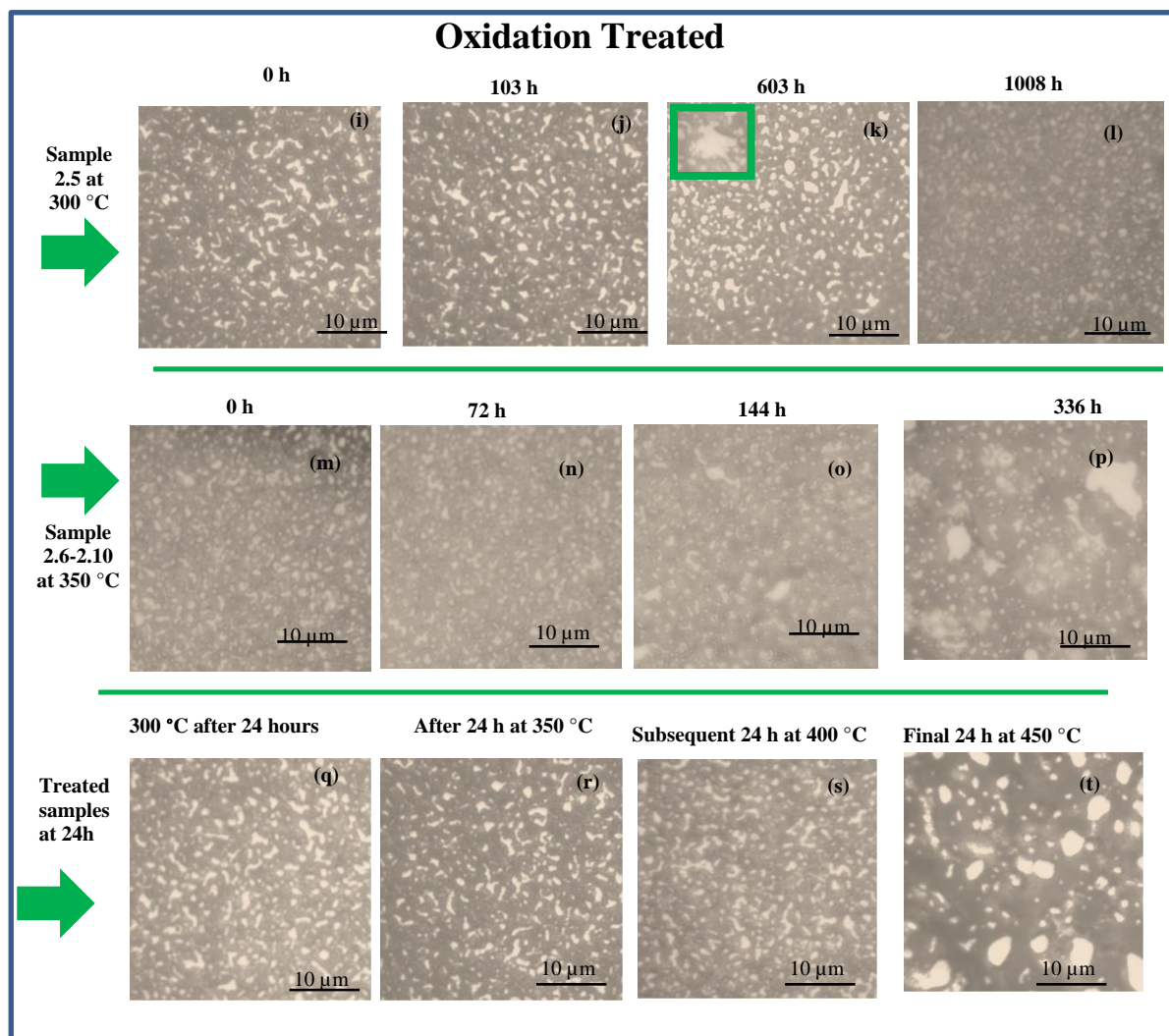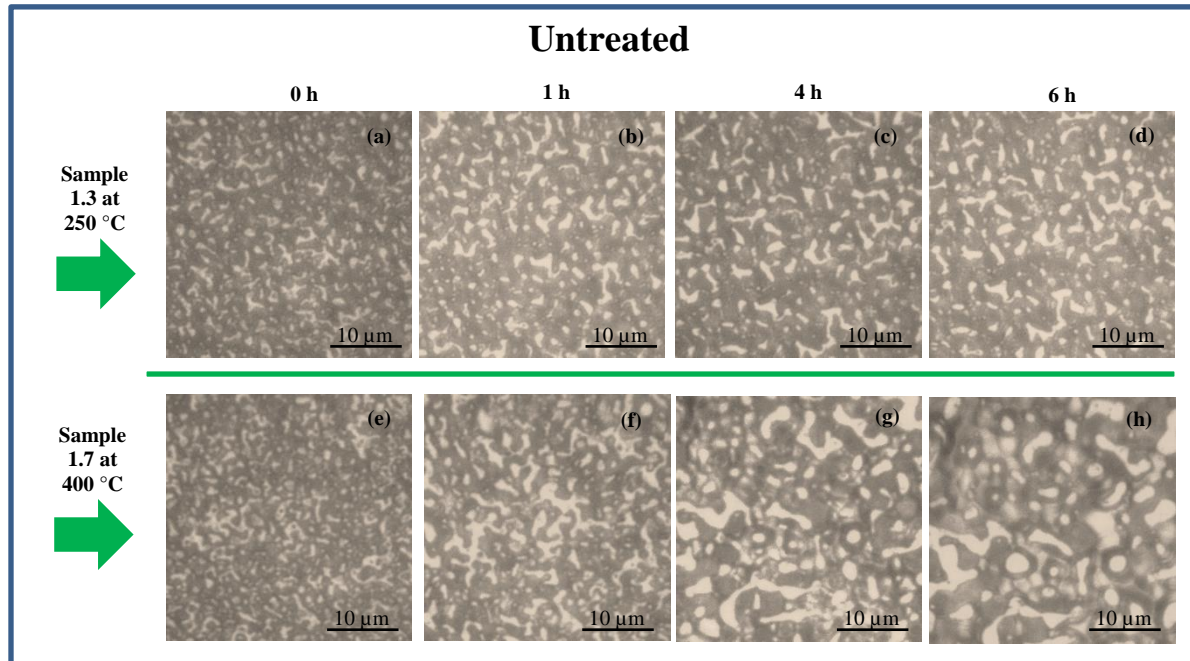
Untreated

	0 h	1 h	4 h	6 h

Sample 1.3 at 250 °C

(a) 10 µm (b) 10 µm (c) 10 µm (d) 10 µm

Sample 1.7 at 400 °C

(e) 10 µm (f) 10 µm (g) 10 µm (h) 10 µm

Oxidation Treated

	0 h	103 h	603 h	1008 h

Sample 2.5 at 300 °C

(i) 10 µm (j) 10 µm (k) 10 µm (l) 10 µm

	0 h	72 h	144 h	336 h

Sample 2.6-2.10 at 350 °C

(m) 10 µm (n) 10 µm (o) 10 µm (p) 10 µm

300 °C after 24 hours	After 24 h at 350 °C	Subsequent 24 h at 400 °C	Final 24 h at 450 °C

Treated samples at 24h

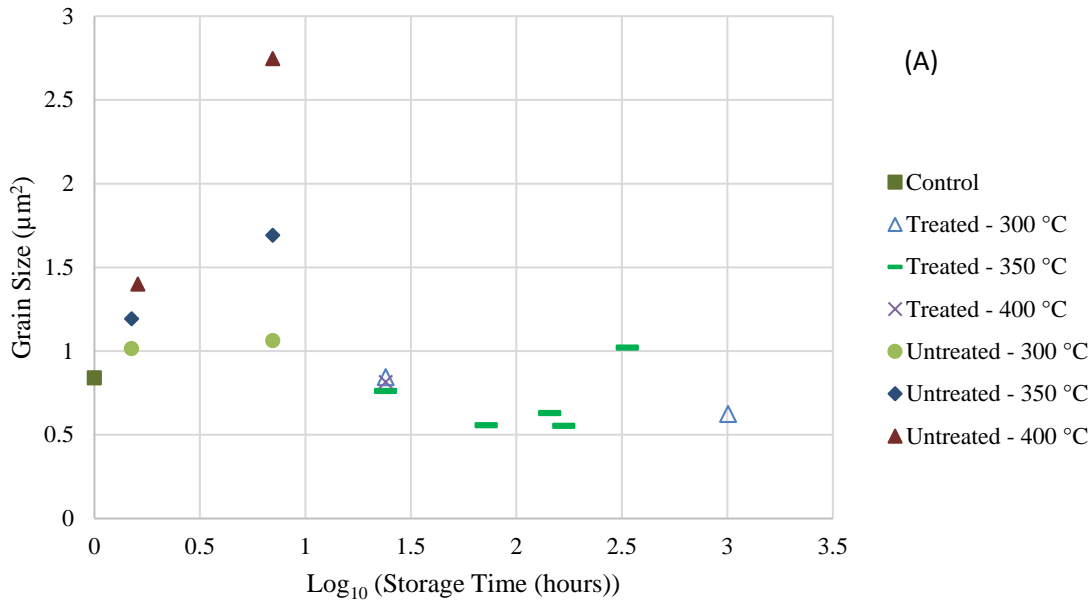(q) 10 µm (r) 10 µm (s) 10 µm (t) 10 µm

12

Fig 4: Comparison of grains sizes of treated and untreated samples. (A) Grain size versus storage time up to 1000 h
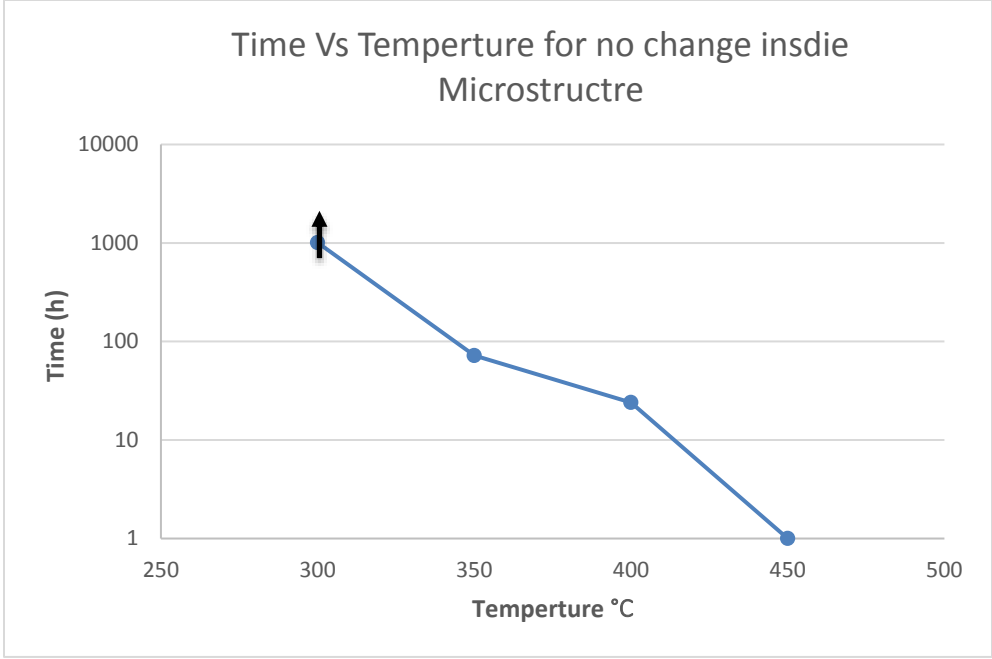
Fig. 5: Microstructure stability duration versus temperature (ultimate duration at 300 °C unknown).
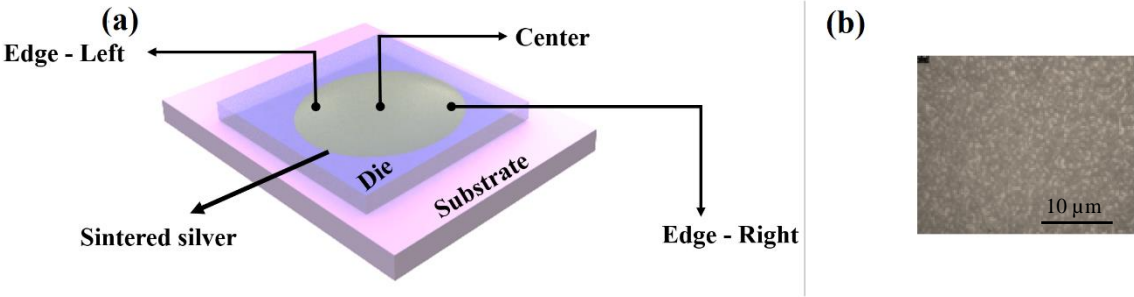

Fig. 6: (a) Layer scheme of the samples showing the different measurements locations. (b) Optical image of the control sample.
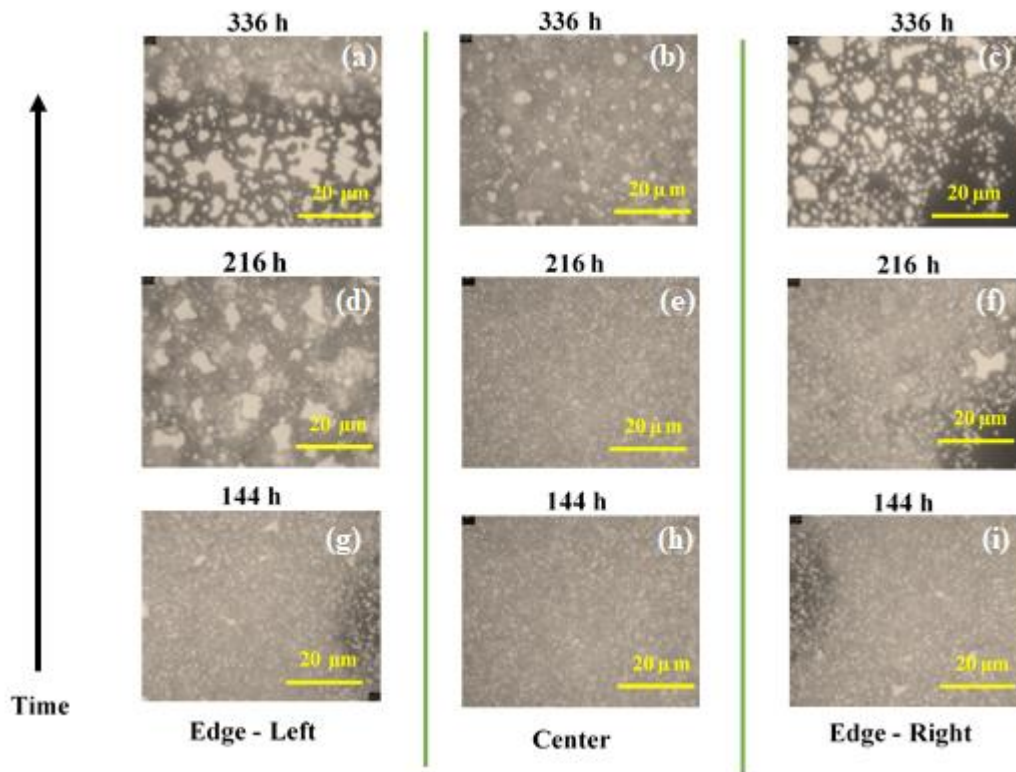
Fig. 7: Optical images of treated sintered silver at 350 °C under cover-slip after storage at different locations and time: (a-c) 336 h, (d-f) 216 h and (g-i) 144 h.
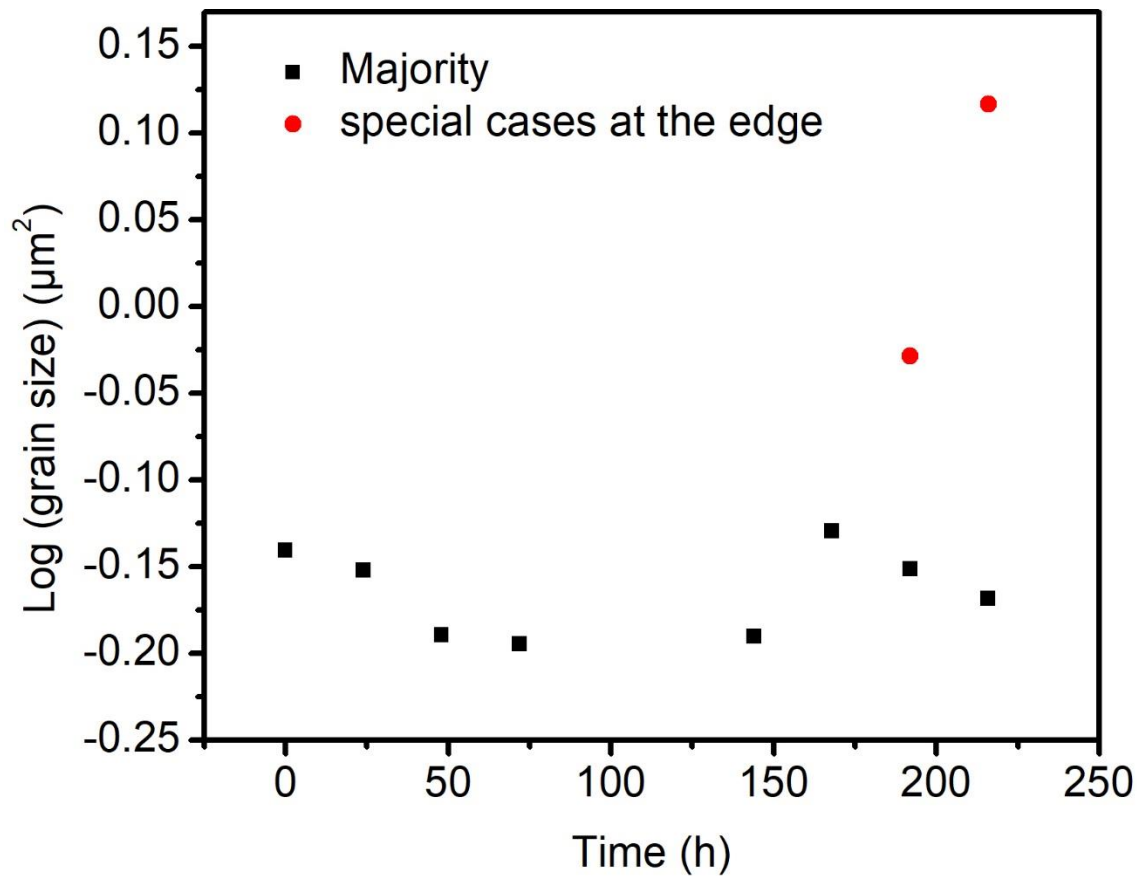
Figure 8: Grain size versus storage duration for the treated samples, stored at 350 °C.

b) COMSOL Simulation

Optical images of the untreated sintered silver structure stored at 387 °C are shown in Fig. 9 (a-h). Some information can be acquired from the evolution of average grain size as presented in section 3a and in previous work [13][6], . However, by investigating the changes in a single grain and tracking the changes, additional information can be acquired about the physical mechanisms that drive the changes. As shown in Fig. 9 (i-l), the overall quantitative changes to the grain structure predicted in the simulation are very similar to the experimental observations in Fig. 9

(e-h). However, the simulated evolution is about 150 times faster than experimental observations. This difference can be explained by the value used for silver surface diffusion coefficient D_S in Eq. 1, which has been referenced from experiments on a clean silver surface [22].
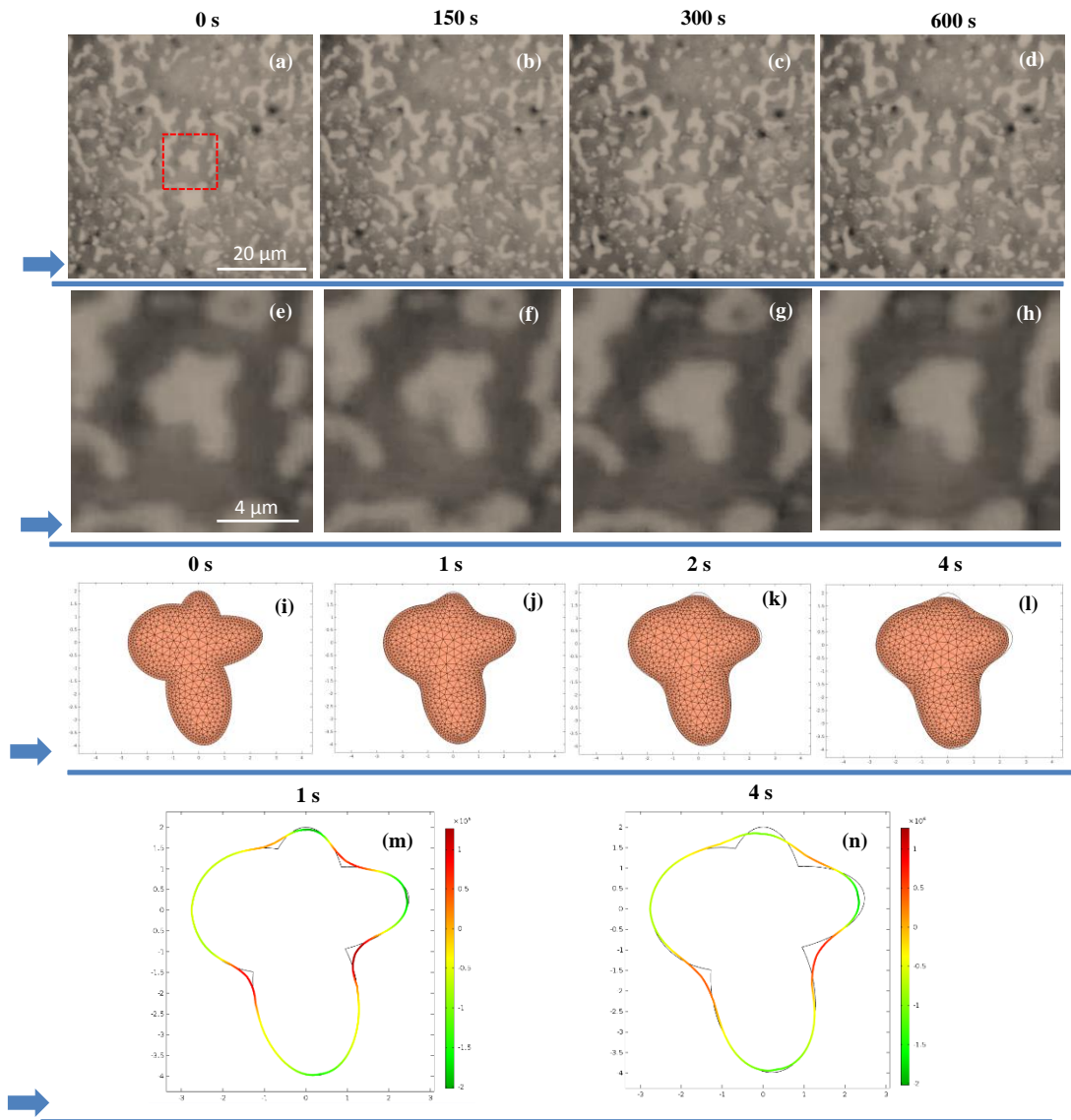

Fig. 9. Microstructural evolution at 387 °C. (a-d) Optical Images of the experimental sample. (e-h) Microstructural evolution of the selected experimental grain. (i-l) Simulation results of the grain's behavior (axes are in micrometer). (m-n) Curvature values on the grain's surface, showing the relaxation over time (axes are in micrometer).

Another tracked grain from the sample stored at 350 °C can be seen in Fig. 10 (a-f). At this

temperature the quantitative microstructural changes observed in the simulation, shown in Fig.

10 (g-i), are again similar to those observed experimentally. However, the simulated grain

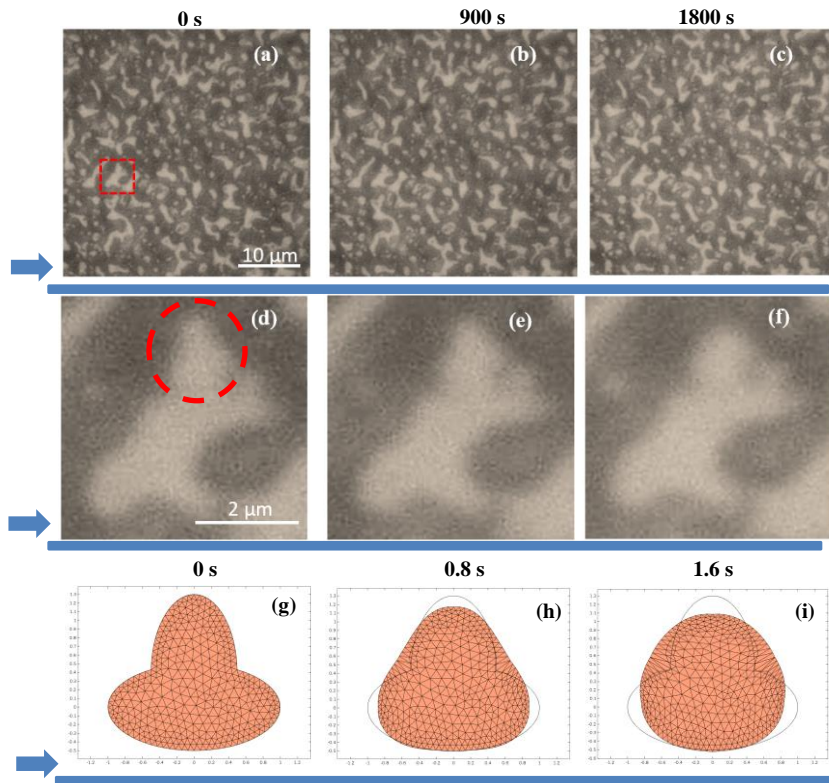evolved about 1125 times faster than experiment.

Fig. 10. Microstructural evolution at 350 °C. (a-c) Optical Images
of the experimental sample. (d-f) Microstructural evolution of the
selected experimental grain inside the red circle. (g-i) Simulation
results of the grain's behavior (axes are in micrometer).

To investigate the cause of the differences in evolution rates DSC analysis has been performed

on the silver paste. As can be seen from Fig. 11, decomposition of the organic materials in the

paste ends at around 360 °C. Below this temperature, for example, for the 350 °C aged sample,

solvents and ligands may be present and adsorbed onto the surface of the silver, resulting in the

three orders of magnitude evolution rate suppression observed. For the 387 °C sample the

organics will have decomposed but the remaining two orders of magnitude suppression would then be related to compounds such as silver oxide. The decomposition temperature of one silver oxide is approximately 400 °C [25], while others decompose at higher temperature. It is notable that in previous work, it has been shown that below 400 °C sintered silver morphology evolution can be completely arrested by exposure of the pore surfaces to air, while above 400 °C exposure to air no longer arrests the evolution and grains transform rapidly[6]. Hence the slowdown of changes at 387 °C, which is a random temperature between the 360 °C decomposition temperature and faster grain growth at 400 °C, may be due to residual oxygen in the pores or air penetration through the porous silver causing partial oxidation of the silver surface in the pores. It is known that extremely slight oxidization of silver can result in enhancement of surface diffusion [26] [27], while heavy oxidation by exposure to air stops surface diffusion and grain growth up to 400 °C [28]. The partial arrest seen in the experiments seems therefore to be linked to moderate oxidation of the silver surface. It is possible to propose that the steam treatment and other oxidizing treatments in Table 1 convert the lightly oxidized surface which is already present into a completely oxidized surface.
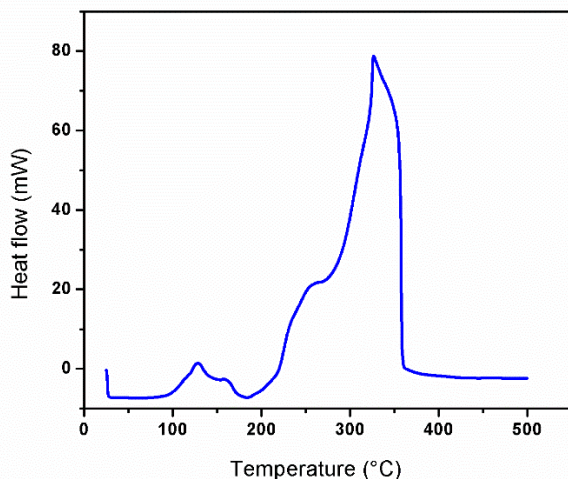

Fig. 11. DSC of the silver paste from room temperature to 500 °C.

3c) XPS Results

The XPS technique has been utilized to examine the initial chemical state of the samples after sintering. Fig.12(a) shows clear peaks of C 1s, Ag 3d, O 1s, Ag 3P, Ag 3p$_{1/2}$, and Ag 3s at binding energies of 284.47 eV, 369.78 eV, 531.34 eV, 584.8 eV, 605.73 eV, 718.5 eV, respectively. However, other peaks (without labels) are due to the trace materials in the samples. The high resolution XPS scan shown in Fig.12 (b) reveals the formation of Ag$_2$O with two peaks splits into two binding energies. A Gaussian-Lorentzian symmetric fitting was applied on the detected peaks to calculate the average binding energies. The calculated binding energies of 368.48 eV and 374.47 eV are corresponding to Ag 3d$_{5/2}$ and Ag 3d$_{3/2}$ excitations, respectively. These results give further evidence that a pre-existing silver oxide Ag$_2$O exists on the surface after the sintering process, and even before the steam treatment is applied. The XPS method is not particularly well suited to determining the level of oxide present as differing ageing results show randomly varying peak strengths.
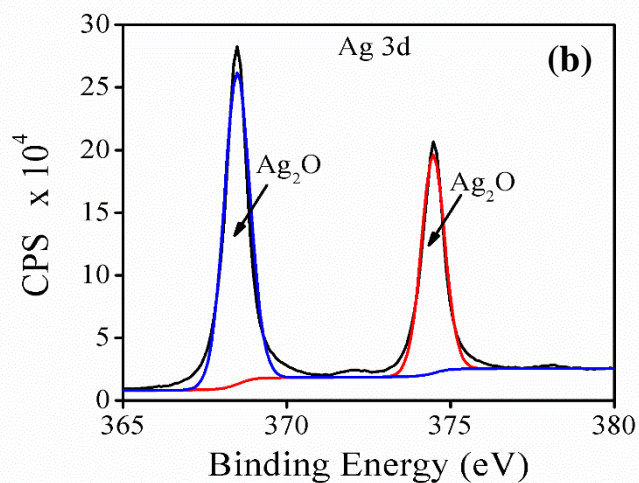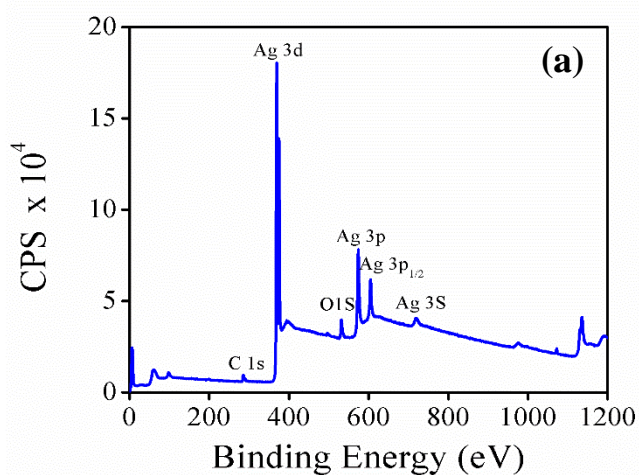
Fig.12: (a) XPS spectrum of sintered Ag treated sample by sintering process at 255 °C for 25 minutes. **(b)** Ag 3d High resolution XPS spectrum of sintered Ag treated sample. [New without cover slip]

4. Conclusions:

The steaming technique can prevent the changes even for at least 1008 h at 300 °C, and at most 72 h at 350 °C and 24 h at 400 °C hours while no effective prevention is observable at higher temperatures. While the standard steaming condition of steam exposure at 150 °C was chosen to ensure good penetration of steam into the sintered silver, the experiments have shown that shorter exposures of only 1 h, or even just immersion into water for 10 minutes before high temperature storage provide an effective barrier layer. The treatment can be applied by using oxidizing agents such as hydrogen peroxide. The simulation of untreated sintered silver grain growth at high temperatures shows the presence of coatings on the surface of the silver in the interior pores, which are responsible for reducing the speed of grain growth and microstructural evolution. The high resolution XPS measurements confirm the formation of silver oxide (Ag2O) in the as-sintered samples and it is hypothesized that the steaming technique converts the partially oxidized surface into a fully oxidized surface. The mechanism for barrier breakdown at temperatures above 300 °C has not been determined, but breakdown has been shown to occur progressively from the edges of the sample. Further investigation of the breakdown mechanism using XPS data from a much larger sample set would help to identify the exact mechanism. Irrespective of the mechanism, our results show that die attach joint microstructure can be stabilized at temperatures up to 300 °C resulting in more stable and predictable joint properties.

REFERENCES:

[1]   V. R. V. R. Manikam and K. Y. K. Y. K. Y. Cheong, "Die Attach Materials for High Temperature Applications: A Review," *Components, Packag. Manuf. Technol. IEEE Trans.*, vol. 1, no. 4, pp. 457–478, 2011.

[2]   K. S. Tan and K. Y. Cheong, "Mechanical properties of sintered Ag-Cu die-attach nanopaste for

application on SiC device," *Mater. Des.*, vol. 64, pp. 166–176, 2014.

[3]   A. Masson, C. Buttay, H. Morel, C. Raynaud, S. Hascoet, and L. Gremillard, "High-temperature die-attaches for SiC power devices," *Proc. 14th Eur. Conf. Power Electron. Appl.*, pp. 1–10, 2011.

[4]   T. A. Tollefsen, O. M. Løvvik, K. Aasmundtveit, and A. Larsson, "Effect of temperature on the die shear strength of a Au-Sn SLID bond," *Metall. Mater. Trans. A Phys. Metall. Mater. Sci.*, vol. 44, no. 7, pp. 2914–2916, 2013.

[5]   S. A. Paknejad and S. H. Mannan, "Review of silver nanoparticle based die attach materials for high power/temperature applications," *Microelectron. Reliab.*, vol. 70, pp. 1–11, 2017.

[6]   S. A. Paknejad, A. Mansourian, J. Greenberg, K. Khtatba, L. Van Parijs, and S. H. Mannan, "Microstructural evolution of sintered silver at elevated temperatures," *Microelectron. Reliab.*, vol. 63, pp. 125–133, 2016.

[7]   K. S. Siow, "Are sintered silver joints ready for use as interconnect material in microelectronic packaging?," *J. Electron. Mater.*, vol. 43, no. 4, pp. 947–961, 2014.

[8]   S. A. Paknejad, A. Mansourian, Y. Noh, K. Khtatba, and S. H. Mannan, "Thermally stable high temperature die attach solution," *Mater. Des.*, vol. 89, pp. 1310–1314, 2016.

[9]   H. Zhang, S. Nagao, and K. Suganuma, "Addition of SiC Particles to Ag Die-Attach Paste to Improve High-Temperature Stability; Grain Growth Kinetics of Sintered Porous Ag," *J. Electron. Mater.*, vol. 44, no. 10, pp. 3896–3903, 2015.

[10]   S. A. Paknejad, K. Khtatba, A. Mansourian, and S. H. Mannan, "Ultra-Stable Sintered Silver Die Attach for Demanding High-Power/Temperature Applications," *IEEE Trans. Device Mater. Reliab.*, vol. 17, no. 4, pp. 795–798, 2017.

[11]   I. Conference, "International Conference and Exhibition on High Temperature Electronics Network (HiTEN) | July 10-12, 2017 | Cambridge, UK," 2017.

[12]   S. L. Burkett, M. Zeee, E. M. Charlson, E. J. Charlson, H. K. Yasuda, and D. Yang, "The Effect of Cleaning Procedures on Surface Charging of Various Substrates," vol. 8, no. 1, 1995.

[13]   S. A. Paknejad, "Factors influencing microstructural evolution in nanoparticle sintered Ag die

attach," pp. 50–58, 2015.

[14] F. Le Henaff, S. Azzopardi, E. Woirgard, T. Youssef, S. Bontemps, and J. Joguet, "Lifetime Evaluation of Nanoscale Silver Sintered Power Modules for Automotive Application Based on Experiments and Finite-Element Modeling," *IEEE Trans. Device Mater. Reliab.*, vol. 15, no. 3, pp. 326–334, 2015.

[15] M. W. Reiterer and K. G. Ewsuk, "An analysis of four different approaches to predict and control sintering," *J. Am. Ceram. Soc.*, vol. 92, no. 7, pp. 1419–1427, 2009.

[16] F. Wakai, "Modeling and simulation of elementary processes in ideal sintering," *J. Am. Ceram. Soc.*, vol. 89, no. 5, pp. 1471–1484, 2006.

[17] L. Ding, R. L. Davidchack, and J. Pan, "A molecular dynamics study of sintering between nanoparticles," *Comput. Mater. Sci.*, vol. 45, no. 2, pp. 247–256, 2009.

[18] H. N. Ch'ng and J. Pan, "Modelling microstructural evolution of porous polycrystalline materials and a numerical study of anisotropic sintering," *J. Comput. Phys.*, vol. 204, no. 2, pp. 430–461, 2005.

[19] H. N. Ch'ng and J. Pan, "Sintering of particles of different sizes," *Acta Mater.*, vol. 55, no. 3, pp. 813–824, 2007.

[20] H. Matsubara, "Computer simulations for the design of microstructural developments in ceramics," *Comput. Mater. Sci.*, vol. 14, no. 1–4, pp. 125–128, 1999.

[21] A. M. Ferraria, A. P. Carapeto, and A. M. Botelho Do Rego, "X-ray photoelectron spectroscopy: Silver salts revisited," *Vacuum*, vol. 86, no. 12, pp. 1988–1991, 2012.

[22] C. G. Turuelo, B. Bergmann, and C. Breitkopf, "Void Shape Evolution of Silicon Simulation : Non-linear Three-dimensional Curvature Calculation by First Order Analysis," vol. 2, pp. 27–45, 2014.

[23] S. A. Paknejad, G. Dumas, G. West, G. Lewis, and S. H. Mannan, "Microstructure evolution during 300 °c storage of sintered Ag nanoparticles on Ag and Au substrates," *J. Alloys Compd.*, vol. 617, pp. 994–1001, 2014.

[24] W. Rmili, N. Vivet, S. Chupin, T. Le Bihan, G. Le Quilliec, and C. Richard, "Quantitative Analysis

of Porosity and Transport Properties by FIB-SEM 3D Imaging of a Solder Based Sintered Silver for a New Microelectronic Component," *J. Electron. Mater.*, vol. 45, no. 4, pp. 2242–2251, 2016.

[25]   T. Morita, Y. Yasuda, E. Ide, Y. Akada, and A. Hirose, "Bonding Technique Using Micro-Scaled Silver-Oxide Particles for <I>In-Situ</I> Formation of Silver Nanoparticles," *Mater. Trans.*, vol. 49, no. 12, pp. 2875–2880, 2008.

[26]   A. R. Layson, J. W. Evans, and P. A. Thiel, "Additive-enhanced coarsening and smoothening of metal films: Complex mass-flow dynamics underlying nanostructure evolution," *Phys. Rev. B - Condens. Matter Mater. Phys.*, vol. 65, no. 19, pp. 1–4, 2002.

[27]   G. . Rhead, "Surface self-diffusion of silver in various atmospheres," *Acta Metall.*, vol. 13, no. 3, pp. 223–226, Mar. 1965.

[28]   R. Dannenberg, E. Stach, J. R. Groza, and B. J. Dresser, "TEM annealing study of normal grain growth in silver thin films," *Thin Solid Films*, vol. 379, no. 1–2, pp. 133–138, 2000.